

Gravity induced evolution of a magnetized fermion gas with finite temperature

I. Delgado Gaspar[♣], A. Pérez Martínez[◇], Roberto A. Sussman[♠] and A. Ulacia Rey^{◇,♠}.

[♣] Instituto de Geofísica y Astronomía (IGA). Calle 212 No 2906, La Lisa. La Habana, Cuba. cp-11600.

[◇] Instituto de Cibernética, Matemática, y Física (ICIMAF). Calle 15 No. 309, Vedado. La Habana, Cuba. cp-10400.

[♠] Instituto de Ciencias Nucleares, Universidad Nacional Autónoma de México (ICN-UNAM). A. P. 70-543, 04510 México D. F.

E-mail: [♣]idelgado@iga.cu, [◇]aurora@icimaf.cu ,

[♠]sussman@nucleares.unam.mx,

^{◇,♠}alainulacia@nucleares.unam.mx/alain@icimaf.cu

Abstract. We examine the near collapse dynamics of a self-gravitating magnetized electron gas at finite temperature, taken as the source of a Bianchi-I spacetime described by the Kasner metric. The set of Einstein–Maxwell field equations reduces to a complete and self-consistent system of non-linear autonomous ODE’s. By considering a representative set of initial conditions, the numerical solutions of this system show the gas collapsing into both, isotropic (“point-like”) and anisotropic (“cigar-like”) singularities, depending on the intensity of the magnetic field. We also examined the behavior during the collapse stage of all relevant state and kinematic variables: the temperature, the expansion scalar, the magnetic field, the magnetization and energy density. We notice a significant qualitative difference in the behavior of the gas for a range of temperatures between the values $T \sim 10^3\text{K}$ and $T \sim 10^7\text{K}$.

PACS numbers: 98.80.-k, 04.20.-q, 04.40.+b, 05.30.Fk, 95.36.+x, 95.35.+d

1. Introduction

Astrophysical systems provide an ideal scenario to examine the effects of strong magnetic fields associated with self-gravitating sources under critical conditions. In such conditions, we expect non-trivial coupling between gravitation and other fundamental interactions (strong, weak and electromagnetic), and from this interplay important clues of their unification could emerge.

The presence and effects of strong magnetic fields in compact objects (neutron, hybrids and quark stars) have been studied in the literature (see [1, 2, 3, 4, 5, 6, 7, 8], and references quoted therein), assuming various types of equations of state (EOS) has been obtained and considering in some of these papers numerical solutions of the equilibrium Tolman–Oppenheimer–Volkov (TOV) equation.

As proven in previous work [1, 8, 9, 10, 11], the presence of a magnetic field is incompatible with spherical symmetry and necessarily introduces anisotropic pressures. However, by assuming that anisotropies and deviations from spherical symmetry remain small, several authors [8, 10, 12] have managed to compute observable quantities of idealized static and spherical compact objects under the presence of strong magnetic fields by means of TOV equations that incorporate these anisotropic pressures. Moreover, it is evident that much less idealized models would result by considering the magnetic field and its associated pressure anisotropies in the context of TOV equations under axial symmetric (or at least cylindrically symmetric) geometries [8].

As an alternative (though still idealized) approach, and bearing in mind the relation between magnetic fields and pressure anisotropy, we have examined the dynamics of magnetized self-gravitating Fermi gases as sources of a Bianchi I space-time [13, 14, 15], as this is the simplest non-stationary geometry that is fully compatible with a the anisotropy produced by a magnetic field source.

Evidently, a Bianchi I model is a completely inadequate metric for any sort of a compact object, as all geometric and physical variables depend only on time (and thus it cannot incorporate any coupling of gravity with spatial gradients of these variables). However, the use of this idealized geometry could still be useful to examine qualitative features of the local behavior of the magnetized gas under special and approximated conditions. Specifically, we aim at providing qualitative results that could yield a better understanding of the conditions approximately prevailing near the center and the rotation axis of less idealized configurations, where the angular momentum of the vorticity and the spatial gradients of the 4-acceleration and other key variables play a minor dynamical role.

The main objective of the present paper is to include the effect of the temperature in the study that we accomplished in [13]. We aim at addressing the question of whether a finite temperature produces a significant dynamical effect in “slowing down” or reversing the evolution of the magnetized gas in the collapsing regime, as such qualitative difference may be related to the stability of the self-gravitating configuration. We also analyze the relations between the magnetization and magnetic field, and the energy density and temperature.

The paper is organized as follow. In section II we derive the EOS for a dense magnetized electron gas at finite temperature. In section III we lay out the dynamical equations for the evolution of our model by writing up the Einstein–Maxwell system of equation for the specific source under consideration. Einstein–Maxwell equations are written in section IV as a system of non-linear autonomous differential equations,

rewriting it in section V in terms of physically motivated dimensionless variables. The numerical analysis of the collapsing solutions and the discussion of the physical results are given in the section VI. Our conclusions are presented in sections VII.

2. Magnetized Fermi gas as a source of a Bianchi I background geometry

Homogeneous but anisotropic Bianchi I models are described by the Kasner metric

$$ds^2 = -dt^2 + Q_1(t)^2 dx^2 + Q_2(t)^2 dy^2 + Q_3(t)^2 dz^2, \quad (1)$$

so that spatial curvature vanishes and all quantities depend only on time. Assuming a comoving frame with coordinates $x^a = [t, x, y, z]$ and 4-velocity $u^a = \delta_t^a$, the energy-momentum tensor for a self-gravitating magnetized gas of free electrons is given by:

$$T_b^a = (U + P) u^a u_b + P \delta_b^a + \Pi_b^a, \quad P = p - \frac{2BM}{3}, \quad (2)$$

where B is the magnetic field (pointing in the z direction), U is the energy density (including the rest energy of the electrons), M is the magnetization of the gas, P is the isotropic pressure and Π_b^a is the traceless anisotropic pressure tensor:

$$\Pi_b^a = \text{diag} [\Pi, \Pi, -2\Pi, 0], \quad \Pi = -\frac{BM}{3}, \quad (3)$$

We can write the energy-momentum (2) tensor as:

$$T_b^a = \text{diag} [-U, P_\perp, P_\perp, P_\parallel], \quad (4)$$

which respectively identifies P_\perp and P_\parallel as the pressure components perpendicular and parallel to the magnetic field. Notice that the anisotropy in T_b^a is produced by the magnetic field B . If this field vanishes, the energy-momentum tensor reduces to that of a perfect fluid with isotropic pressure (an ideal gas of electrons complying with Fermi-Dirac statistics).

The equations of state for this magnetized electron gas can be given in the following form [16]:

$$\begin{aligned} P_\parallel = -\Omega &= \lambda \beta \left[\frac{1}{2} C_2(\phi, \mu) + \sum_{n=1}^{\infty} a_n^2 C_2 \left(\frac{\phi}{a_n}, \frac{\mu}{a_n} \right) \right] \\ &\equiv \lambda \Gamma_\parallel(\beta, \mu, \phi), \end{aligned} \quad (5)$$

$$P_\perp = \lambda \beta^2 \sum_{n=1}^{\infty} n C_1 \left(\frac{\phi}{a_n}, \frac{\mu}{a_n} \right) \equiv \lambda \Gamma_\perp(\beta, \mu, \phi), \quad (6)$$

$$U = \lambda \beta \left[\frac{1}{2} C_3(\phi, \mu) + \sum_{n=1}^{\infty} a_n^2 C_3 \left(\frac{\phi}{a_n}, \frac{\mu}{a_n} \right) \right] \equiv \lambda \Gamma_U(\beta, \mu, \phi). \quad (7)$$

The particle number density is,

$$\eta = \frac{\lambda}{m_e} \beta \left[\frac{1}{2} C_4(\phi, \mu) + \sum_{n=1}^{\infty} a_n C_4 \left(\frac{\phi}{a_n}, \frac{\mu}{a_n} \right) \right] \equiv \frac{\lambda}{m_e} \Gamma_\eta(\beta, \mu, \phi), \quad (8)$$

with $a_n = \sqrt{1 + 2n\beta}$ and C_1, C_2, C_3, C_4 are given by:

$$C_1(\phi, \mu) = \int_0^\infty \frac{1}{1 + \exp\left(\frac{\sqrt{1+x^2}-\mu}{\phi}\right)} \frac{dx}{\sqrt{1+x^2}}, \quad (9)$$

$$C_2(\phi, \mu) = \int_0^\infty \frac{x^2}{1 + \exp\left(\frac{\sqrt{1+x^2}-\mu}{\phi}\right)} \frac{dx}{\sqrt{1+x^2}}, \quad (10)$$

$$C_3(\phi, \mu) = \int_0^\infty \frac{\sqrt{1+x^2}}{1 + \exp\left(\frac{\sqrt{1+x^2}-\mu}{\phi}\right)} dx, \quad (11)$$

$$C_4(\phi, \mu) = \int_0^\infty \frac{1}{1 + \exp\left(\frac{\sqrt{1+x^2}-\mu}{\phi}\right)} dx. \quad (12)$$

The equations (5) and (6) can be accommodated as [9, 17]:

$$P_\perp = P_\parallel - BM, \quad (13)$$

where M , the magnetization, can be written in the following form:

$$M = M_0 \Gamma_M(\beta, \mu, \phi), \quad (14)$$

with $M_0 = 2\pi\mu_B/(\lambda_c^3)$ and Γ_M is obtained of the expressions (5), (6) and (13).

In the previous expressions μ is the dimensionless chemical potential normalized by the rest energy, $\phi = kT/m_e$, $\beta = B/B_c$, where $B_c = 4.414 \times 10^{13}$ G is the critical magnetic field, μ_B is the Bohr magneton and $\lambda = 8\pi m_e/(\lambda_c^3)$ where λ_c is the Compton wavelength of the electron.

In Appendix A the integrals (9)–(12) have been transformed into equivalent expressions in order to facilitate the numerical calculations.

3. Einstein–Maxwell equations

Since we are interested in the critical relativistic regimen, the dynamics of the magnetized gas whose EOS we have described in the previous section must be studied through the Einstein field equations in the framework of General Relativity:

$$G_{\mu\nu} = R_{\mu\nu} - \frac{1}{2}Rg_{\mu\nu} = \kappa T_{\mu\nu}, \quad (15)$$

together with the balance equations of the energy–momentum tensor and Maxwell’s equations,

$$T^{\mu\nu}{}_{;\nu} = 0, \quad (16)$$

$$F^{\mu\nu}{}_{;\nu} = 0, \quad F_{[\mu\nu;\alpha]} = 0, \quad (17)$$

where $\kappa = 8\pi G_N$ and G_N is Newton’s gravitational constant, while square brackets denote anti-symmetrization in (17).

Assuming absence of annihilation/creation processes, so that particle numbers are conserved, leads to the following conservation equation:

$$n^\alpha{}_{;\alpha} = 0, \quad n^\alpha = \eta u^\alpha, \quad (18)$$

where η is the particle number density. From the field equations (15) we obtain:

$$-G^x_x = \frac{\dot{Q}_2\dot{Q}_3}{Q_2Q_3} + \frac{\ddot{Q}_2}{Q_2} + \frac{\ddot{Q}_3}{Q_3} = -\kappa P_\perp, \quad (19)$$

$$-G^y_y = \frac{\dot{Q}_1\dot{Q}_3}{Q_1Q_3} + \frac{\ddot{Q}_1}{Q_1} + \frac{\ddot{Q}_3}{Q_3} = -\kappa P_\perp, \quad (20)$$

$$-G_z^z = \frac{\dot{Q}_1 \dot{Q}_2}{Q_1 Q_2} + \frac{\ddot{Q}_1}{Q_1} + \frac{\ddot{Q}_2}{Q_2} = -\kappa P_{\parallel}, \quad (21)$$

$$-G_t^t = \frac{\dot{Q}_1 \dot{Q}_2}{Q_1 Q_2} + \frac{\dot{Q}_1 \dot{Q}_3}{Q_1 Q_3} + \frac{\dot{Q}_2 \dot{Q}_3}{Q_2 Q_3} = \kappa U. \quad (22)$$

where $\dot{Q} = Q_{;\alpha} u^\alpha = Q_{,t}$. From the conservation of the energy–momentum tensor (16) we obtain:

$$\dot{U} = - \left(\frac{\dot{Q}_1}{Q_1} + \frac{\dot{Q}_2}{Q_2} \right) (P_{\perp} + U) - \frac{\dot{Q}_3}{Q_3} (P_{\parallel} + U). \quad (23)$$

Maxwell's equations (17) yield:

$$\frac{\dot{Q}_1}{Q_1} + \frac{\dot{Q}_2}{Q_2} + \frac{1}{2} \frac{\dot{B}}{B} = 0, \quad (24)$$

and from the particle number conservation (18) leads to:

$$\dot{\eta} + \left(\frac{\dot{Q}_1}{Q_1} + \frac{\dot{Q}_2}{Q_2} + \frac{\dot{Q}_3}{Q_3} \right) \eta = 0. \quad (25)$$

4. Local kinematic variables

Einstein–Maxwell field equations are second order system of ordinary differential equations (ODE's). In order to work with a first order system of ODE's, it is useful and convenient to rewrite these equations in terms of covariant kinematic variables that convey the geometric effects on the kinematics of local fluid elements through the covariant derivatives of u^α . For a Kasner metric in the comoving frame endowed with a normal geodesic 4–velocity, the only non–vanishing kinematic parameters are the expansion scalar, Θ , and the shear tensor $\sigma_{\alpha\beta}$:

$$\Theta = u^\alpha{}_{;\alpha}, \quad \sigma_{\alpha\beta} = u_{(\alpha;\beta)} - \frac{\Theta}{3} h_{\alpha\beta}, \quad (26)$$

where $h_{\alpha\beta} = u_\alpha u_\beta + g_{\alpha\beta}$ is the projection tensor and rounded brackets denote symmetrization. These parameters take the form:

$$\Theta = \frac{\dot{Q}_1}{Q_1} + \frac{\dot{Q}_2}{Q_2} + \frac{\dot{Q}_3}{Q_3}, \quad (27)$$

$$\sigma_\beta^\alpha = \text{diag} [\sigma_x^x, \sigma_y^y, \sigma_z^z, 0] = \text{diag} [\Sigma_1, \Sigma_2, \Sigma_3, 0], \quad (28)$$

where:

$$\Sigma_a = \frac{2}{3} \frac{\dot{Q}_a}{Q_a} - \frac{1}{3} \frac{\dot{Q}_b}{Q_b} - \frac{1}{3} \frac{\dot{Q}_c}{Q_c}, \quad a \neq b \neq c \ (a, b, c = 1, 2, 3). \quad (29)$$

The geometric interpretation of these parameters is straightforward: Θ represents the isotropic rate of change of the 3–volume of a fluid element, while σ_β^α describes its rate of local deformation along different spatial directions given by its eigenvectors. Since the shear tensor is traceless: $\sigma_\alpha^\alpha = 0$, it is always possible to eliminate any one of the three quantities $(\Sigma_1, \Sigma_2, \Sigma_3)$ in terms of the other two. We choose to eliminate Σ_1 as a function of (Σ_2, Σ_3) . By using equations (27) and (29) we can re–write the second derivatives of the metric functions in (19), (20) y (21) as first order derivatives of Θ ,

Σ_2 and Σ_3 . After some algebraic manipulations it is possible to transform equations (19)-(25) as a first order system of autonomous ODE's:

$$\dot{\Sigma}_2 = \frac{\varkappa}{3} (P_\perp - P_\parallel) - \Theta \Sigma_2, \quad (30a)$$

$$\dot{\Sigma}_3 = \frac{2\varkappa}{3} (P_\parallel - P_\perp) - \Theta \Sigma_3, \quad (30b)$$

$$\dot{B} = 2B \left(\Sigma_3 - \frac{2}{3} \Theta \right), \quad (30c)$$

$$\dot{\mu} = \frac{1}{\text{Det}} [f_1 \eta_{,T} - f_2 U_{,T}], \quad (30d)$$

$$\dot{T} = \frac{1}{\text{Det}} [f_2 U_{,\mu} - f_1 \eta_{,\mu}], \quad (30e)$$

together with the following constraint:

$$\varkappa U = -(\Sigma_2)^2 - \Sigma_2 \Sigma_3 - (\Sigma_3)^2 + \frac{\Theta^2}{3}, \quad (31)$$

where:

$$\text{Det} \equiv U_{,\mu} \eta_{,T} - U_{,T} \eta_{,\mu}, \quad (32)$$

$$f_1 = \left(\Sigma_3 - \frac{2\Theta}{3} \right) (P_\perp + U) - \left(\Sigma_3 + \frac{\Theta}{3} \right) (P_\parallel + U) - U_{,B} \dot{B}, \quad (33)$$

$$f_2 = \Theta \eta + \eta_{,B} \dot{B}. \quad (34)$$

These first order equations form a complete and self-consistent system whose numeric integration fully determines Σ_2 , Σ_3 , B , μ , T , and thus allows us to study the dynamical evolution of a local volume element of a gas of magnetized electrons.

5. Dynamical equations

By introducing the following dimensionless evolution parameter,

$$H = \frac{\Theta}{3}, \quad \frac{d}{d\tau} = \frac{1}{H_0} \frac{d}{dt}, \quad (35)$$

together with the dimensionless variables,

$$\mathcal{H} = \frac{H}{H_0}, \quad S_2 = \frac{\Sigma_2}{H_0}, \quad S_3 = \frac{\Sigma_3}{H_0}, \quad \beta = \frac{B}{B_c}, \quad \mu = \frac{\tilde{\mu}}{m_e}, \quad (36)$$

where we have denoted by $\tilde{\mu}$ the usual chemical potential and H_0 is a constant with inverse length units that sets the characteristic length scale of the system, which we have chosen as $3H_0^2 = \kappa\lambda \Rightarrow H_0 = 0.86 \times 10^{-10} \text{ m}^{-1}$, so that $1/H_0 \cong 1.15 \times 10^{10} \text{ m}$ is of the order of magnitude of an astronomic unit. It indicates that our simplified model is examined on local scales smaller than cosmic scales. In cosmological sources and models [18] $H_0 = 0.59 \times 10^{-26} \text{ m}^{-1}$ would play the role of the Hubble scale constant, this value is a much greater length scale. The functions S_2 and S_3 are the components of the shear tensor normalized with this scale, while τ is the dimensionless time. Substituting (36) into the system (30a)–(30e) we obtain:

$$S_{2,\tau} = \Gamma_\perp - \Gamma_\parallel - 3\mathcal{H}S_2, \quad (37a)$$

$$S_{3,\tau} = 2(\Gamma_\parallel - \Gamma_\perp) - 3\mathcal{H}S_3, \quad (37b)$$

$$\beta_{,\tau} = 2\beta(S_3 - 2\mathcal{H}), \quad (37c)$$

$$\tilde{\mu},\tau = \frac{1}{\text{Det}} \left(\Gamma_{\eta,\phi} \tilde{f}_1 + \Gamma_{U,\phi} \tilde{f}_2 \right), \quad (37d)$$

$$\phi,\tau = -\frac{1}{\text{Det}} \left(\Gamma_{\eta,\mu} \tilde{f}_1 + \Gamma_{U,\mu} \tilde{f}_2 \right). \quad (37e)$$

while the constraint (31) becomes,

$$3\Gamma_U = -S_2^2 - S_3^2 - S_2 S_3 + 3\mathcal{H}^2, \quad (38)$$

and the auxiliary parameters of the previous system take the form:

$$\tilde{f}_1 = (S_3 - 2\mathcal{H}) (\Gamma_{\perp} - 2\Gamma_{U,\beta}\beta) - (S_3 + \mathcal{H}) \Gamma_{\parallel} - 3\Gamma_U \mathcal{H}, \quad (39a)$$

$$\tilde{f}_2 = 3\mathcal{H}\Gamma_{\eta} + 2\Gamma_{\eta,\beta} (S_3 - 2\mathcal{H}), \quad (39b)$$

$$\text{Det} = \Gamma_{U,\mu} \Gamma_{\eta,\phi} - \Gamma_{U,\phi} \Gamma_{\eta,\mu}. \quad (39c)$$

In the following section we undertake the numerical study of this system, focusing concretely in the the collapsing regime.

6. Numeric analysis and physical interpretation

Since the energy–momentum tensor (4) takes the perfect fluid form ($P_{\parallel} = P_{\perp}$) for zero magnetic field, we can identify the magnetic field as the factor introducing anisotropy in the dynamical behavior of the fermionic gas. In particular, this anisotropy in the stress ($P_{\parallel} \neq P_{\perp}$) must yield different evolution in different directions, which must be evident in a critical stage such as the collapsing regime. Intuitively, we expect an isotropic point–like singularity if the pressure is isotropic, as pressure diverges in all direction, but a large pressure anisotropy (which necessarily corresponds to large magnetic field) should lead to a qualitatively different direction dependent critical behavior of the pressure that should result in an anisotropic cigar–like singularity characterized by the divergence of only the pressure parallel to the magnetic field. As we show in figure 1, the pressure parallel and perpendicular for different initial temperatures does exhibit the expected behavior: for initial conditions of small temperatures $\phi(0) = 10^{-7}$ ($\sim 10^3$ K) we have $P_{\parallel} \approx P_{\perp}$ and a point singularity: $P_{\parallel}, P_{\perp} \rightarrow \infty$, but for a larger initial value $\phi(0) = 10^{-4}$ ($\sim 10^6$ K) we have the highly anisotropic evolution $P_{\parallel} \rightarrow \infty$ with $P_{\perp} \rightarrow 0$ that signals a cigar–like singularity (the case $P_{\parallel} = P_{\perp}$ with zero magnetic field is shown as a comparison).

Since $V = \sqrt{-\det g_{\alpha\beta}} = Q_1 Q_2 Q_3$, we obtain by means of (27) and (35) the local volume in terms of \mathcal{H} :

$$V(\tau) = V(0) \exp \left(3 \int_{\tau=0}^{\tau} \mathcal{H} d\tau \right), \quad (40)$$

where we remark that the sign of $\mathcal{H}(\tau)$ implies expansion if $\mathcal{H}(\tau) > 0$, and collapse if $\mathcal{H}(\tau) < 0$. Besides this point, equations (27) and (29) lead to:

$$Q_i(\tau) = Q_i(0) \exp \left[\int_{\tau=0}^{\tau} (\mathcal{H} + S_i) d\tau \right], \quad (i = 1, 2, 3). \quad (41)$$

where $S_1 = -(S_2 + S_3)$.

For the numerical study we assume a magnetized electron gas at high density: $\mu_e(0) = 2$, which means that the chemical potential is $2m_e$. The initial values of the magnetic field and temperature were chosen in the ranges $\beta(0) \sim 10^{-5}$ to $\beta(0) \sim 10^{-4}$

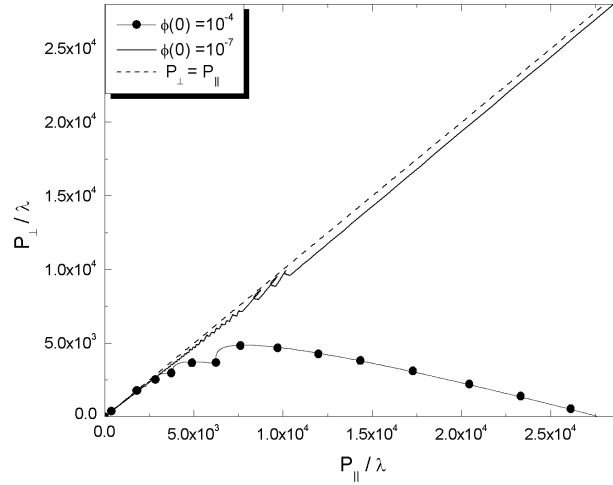


Figure 1. Pressure parallel and perpendicular to the magnetic field. We plot $P_{||}/\lambda$ vs P_{\perp}/λ for initial temperatures $\phi(0) = 10^{-7}, 10^{-4}$ where $\lambda = 8\pi m_e/(\lambda_c^3)$. The case $\beta = 0$ is shown for reference.

and $\phi \sim 10^{-7}$ to $\phi \sim 10^{-3}$ respectively \ddagger Together with $\mathcal{H}(0) < 0$, we consider the conditions $S_2(0) = 0, S_3(0) = 0, +1$, which correspond to the cases with zero initial deformation and initial deformation (shear) in the direction of z axis respectively. The calculation has been done using the fourth-order Runge–Kutta method with the local truncation relative error less than 10^{-6} .

The numerical solutions for the function \mathcal{H} for the assumed values $\mathcal{H}(0)$ show that $\mathcal{H} \rightarrow -\infty$, which implies that the volume element evolves to a singularity (see equation (40)). This is exemplified in figure 2, where numerical solutions are displayed for the expansion scalar. These curves correspond to different values of the initial temperature in the range $\phi(0) = 10^{-7}$ to $\phi(0) = 10^{-3}$, fixing the rest of the initial conditions on the values $\mu(0) = 2, \beta(0) = 5 \times 10^{-5}, S_2(0) = 0$ and $S_3(0) = 1$. Notice that in this regime (as given by these initial conditions) where the high densities are dominant, we do not obtain a direct relation between the values of initial temperatures and the collapse time. In all the configurations the strength of the magnetic field diverges during the collapse of the volume element: this happens independently of the initial conditions. However, the collapsing time diminishes when the values of the initial magnetic field increases, which agrees with the results obtained in [13], where $T = 0$ was assumed.

The expression (41) shows how the evolution of the terms $S_i + \mathcal{H}$ to $\pm\infty$ implies that the metric coefficient Q_i evolves to either $+\infty$ or 0. This evolution is characteristic of an anisotropic “cigar-like” singularity, since two metric coefficients evolve to zero and the third one to $+\infty$, whereas when all metric coefficients tend to zero, the singularity is isotropic “point-like”. See the definitions of these types of singularities

\ddagger Let us remark that $\phi = kT/m_e, \beta = B/B_c$, with $B_c = 4.414 \times 10^{13}\text{G}$ and μ is the chemical potential normalized $\mu_e = \mu_e/m_e$, the magnetic field is in the range $B \sim 10^8\text{G}$ to $B \sim 10^9\text{G}$ and the temperature varies between $T \sim 10^3\text{K}$ and $T \sim 10^7\text{K}$.

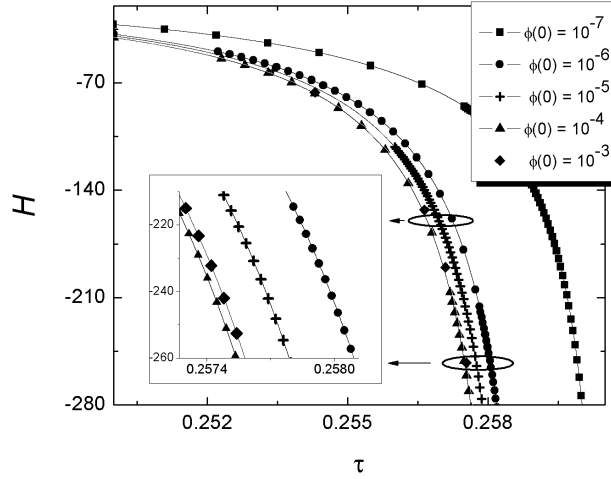


Figure 2. Numerical solutions for the expansion scalar $\mathcal{H}(\tau)$. The box in the lower corner is an amplification of the graphic.

in [19].

For initial conditions with zero shear: $S_1(0) = S_2(0) = S_3(0) = 0$, we always obtain a point-like singularity, independently of the selected values for the remaining initial conditions. However, when the initial deformation is positive in the direction of the magnetic field (z axis), we can obtain either cigar-like or point-like singularities. The nine curves displayed in figure 3 correspond to three sets of functions: $S_i + \mathcal{H}$ ($i = 1, 2, 3$), each one corresponding to these different values of the temperature: $\phi(0) = 10^{-7}, 10^{-6}, 10^{-3}$. All curves were obtained taking as initial conditions: $\mu(0) = 2$, $\beta(0) = 5 \times 10^{-5}$, $S_2(0) = 0$ and $S_3(0) = 1$. For the higher initial values of temperature $\phi(0) = 10^{-6}, 10^{-3}$ the gas collapses into a cigar-like singularity in the direction of the magnetic field, whereas for the lower value $\phi(0) = 10^{-7}$ we obtain a point-like singularity. As expected, an anisotropic singularity occurs as the magnetic field increases, even for relatively low initial temperatures if the initial magnetic field $\beta(0)$ is sufficiently large.

For initial values in the range $\phi(0) \sim 10^{-7}$ to $\phi(0) \sim 10^{-4}$ the temperature decreases as the collapse proceeds, although grows up quickly for values near the collapse time, while for $\phi(0) \sim 10^{-3}$ and higher values it increases.

We display in figure 4 two dashed curves for the evolution of the temperature from the initial value $\phi(0) = 10^{-3}$, together with solid curves that depict temperatures starting at $\phi(0) = 10^{-7}$. In both cases the initial conditions correspond to zero initial shear and positive deformation in the z axis. The initial values of magnetic field and chemical potential were fixed at $\beta(0) = 5 \times 10^{-5}$ and $\mu(0) = 2$ respectively. Notice that the symmetric configuration delays the collapse (yields a longer collapsing time), which may indicate a connection with stability of local fluid elements in compact objects. This could provide an important clue on the stability of a compact object made of a dense magnetized gas. However, verifying this possibility

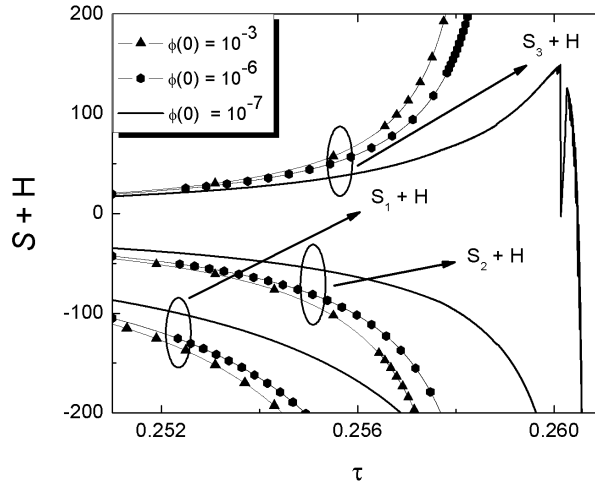


Figure 3. The plots of the functions $S_i + \mathcal{H}$ for $i = 1, 2, 3$. The system has an initial deformation (shear) in the same direction of the magnetic field along the z axis. The collapse is in the form of a “cigar-like” singularity in the z direction for $\phi(0) = 10^{-3}, 10^{-6}$ and a “point-like” singularity for $\phi(0) = 10^{-7}$.

is beyond the scope of this article.

We examine now the behavior of the magnetization and the energy density of the system during the collapse. We remark that the τ -depending functions: β , μ , ϕ follow from the numerical solution of the system (37a)–(37e) and (38), which allows us to compute the magnetization $M(\beta, \mu, \phi)$ and $U(\beta, \mu, \phi)$ for all values of τ . We have depicted curves of M vs. the magnetic field and the energy density vs. temperature \S for initial conditions: $\beta(0) = 5 \times 10^{-5}$, $S_2(0) = S_3(0) = 0$, and for two different values of the initial temperature $\phi(0) = 10^{-7}, 10^{-3}$. These curves are shown in figures 5 and 6.

Notice how at low temperature values the magnetization has an oscillatory behavior with respect to the magnetic field, which correspond to the well known Haas–van Alphen effect [20]. In contrast, for high initial temperatures, the system is heated as the collapse proceeds, with the magnetization behaving monotonically with respect to the magnetic field. These results agree with the study performed in [21], where the authors expressed the magnetization of an electron gas at finite temperature as the sum of two terms: one oscillatory and the other monotonic, which predominate at respectively low and high temperatures.

On the other hand, the energy density increases with the temperature for the initial value $\phi(0) = 10^{-3}$, which does not occurs for the initial value $\phi(0) = 10^{-7}$.

The behavior of the magnetization and the energy density can be explained by taking into account that for the initial value $\phi(0) = 10^{-7}$, as we discussed above, the system is cooled (temperature decreases) during the collapse process with an increasing magnetic field. This is an indication that the effects of the magnetic field

\S Remember that M and U can be written in the following form: $M = M_0 \Gamma_M$ and $U = \lambda \Gamma_U$.

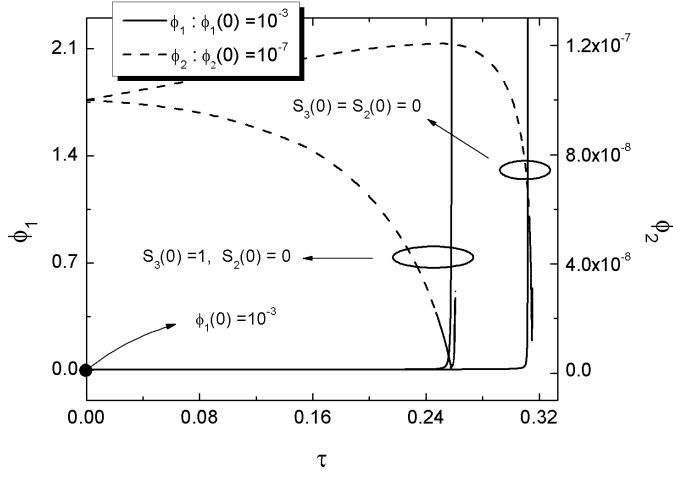


Figure 4. Temperature of the system. The left hand side of the graph displays the temperature values (ϕ_1) corresponding to the two solid curves. The right hand side displays the temperature values (ϕ_2) corresponding to the two dashed curves.

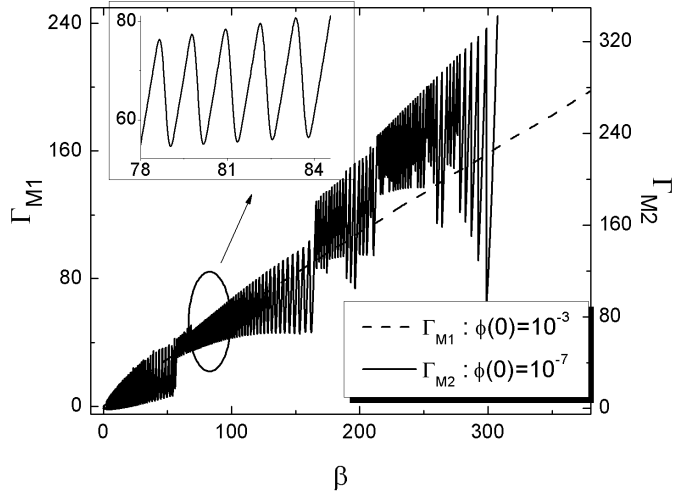


Figure 5. Magnetization versus magnetic field. The axis of the right hand side (Γ_{M2}) depicts the magnetization (the solid curve), while the axis of the left hand side (Γ_{M1}) corresponds to the dashed curve.

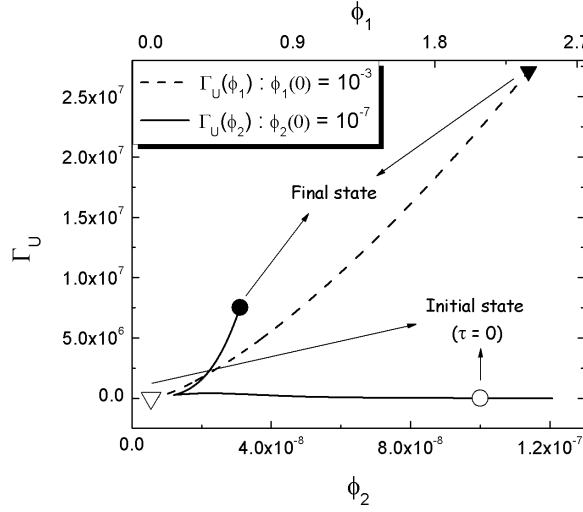


Figure 6. Energy density versus temperature. The temperature values of the curve drawn with solid line should be observed in the lower axis (ϕ_2) and in the top axis (ϕ_1), those of the curve drawn with dashed line.

(alignment of electron spins with the magnetic field) predominate over the effects of temperature (random motion) in the system, a situation in which the Haas–van Alphen oscillations appear in the magnetization curves, with energy density decreasing with temperature in the collapse process. On the other hand, for high initial temperatures ($\phi(0) = 10^{-3}$), the system is heated (temperature increases) during the collapse, which shows the predominance of the effect of temperature over the effect of the field, and showing the magnetization and the energy density following a monotonic behavior with respect to the magnetic field and the temperature, respectively. That is to say, when $\phi(0) \sim 10^{-7}$ the temperature of the system decreases in the collapse process, while the magnetic field increases and the gas evolves to strong magnetic field regimen, where the effect of the temperature is negligible in a first approximation. This is not the case for $\phi(0) \sim 10^{-3}$, for which the temperature rises significantly during the collapse and its effects are significant.

It is worthwhile commenting on the relation between the temperature, magnetic field and magnetization in magnetized gases. In an “earth bound” context when the gas is not self-gravitating, the magnetic field acts as an “external” agent whose effect is to increase the magnetization by aligning the magnetic moments of the electrons. For higher temperatures the internal energy increases and there is more resistance to this effect, resulting in a relatively low magnetization with the electron magnetic moments alignment being relatively random, while at lower temperatures the opposite effect occurs: magnetization is high and magnetic moments strongly align with the magnetic field. However, for a self-gravitating gas the magnetic field is no longer “external”, but generated by the electron magnetic moments themselves, hence the relation between these variables cannot be controlled: it emerges from the dynamics of the gas and depends on the interplay of initial conditions. As we show in

figure 7, a large magnetization coincides with a large magnetic field for relatively low temperatures.

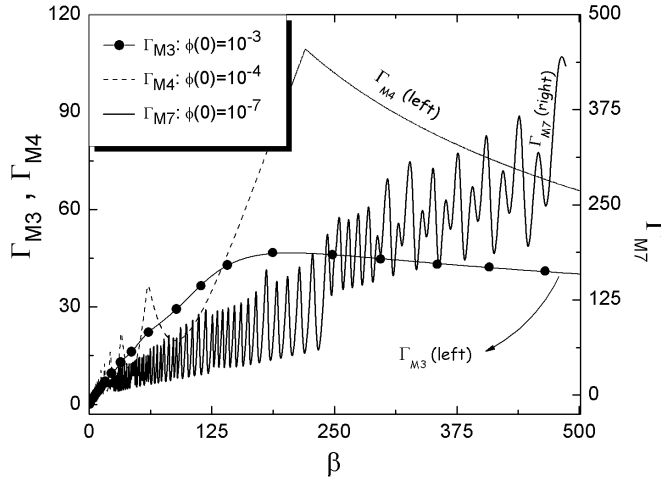


Figure 7. The figure displays the plot of magnetization M for initial temperatures $\phi(0) = 10^{-3}$, 10^{-4} , 10^{-7} and Γ_{M3} , Γ_{M4} (vertical axis in the left hand side) and Γ_{M7} (vertical axis in the right hand side) vs magnetic field β . We considered initial magnetic field $\beta(0) = 5 \times 10^{-5}$ and a positive value for the initial shear component along the z axis (the same value as in the plot of $S + H$ in figure 3). The plots show that larger values for the magnetization correspond to lower temperatures. The case with zero initial shear is displayed in figure 5.

It is important to recall that the study we have undertaken here is based on an equation of state and a thermodynamical potential (Ω) that come from a one-loop approximation. The behavior of the system in the regime ($T^2 \ll eB \ll m_e^2$) may seem strange: the energy density does not increase with the temperature. All this could follow as a consequence that the one-loop approximation may not be appropriate in some regimes for a magnetized system in presence of finite density and temperature. This issue deserves a separate study, possibly in the context of non-perturbative calculations at high magnetic fields, which explore a different approach that may be applicable to the magnetized gas that we have examined here (see [22] and references quoted therein).

7. Conclusion

We have examined the dynamical and thermodynamical behavior of a magnetized, self-gravitating electron gas at finite temperature, taken as the source of a simplified Bianchi I space-time represented by a Kasner metric, which is the simplest geometry that allows us identify the magnetic field as the main source of anisotropy. We regard this configuration as a toy model that roughly approximates a grand canonical subsystem of a magnetized electron source in the conditions prevailing near of the

center and rotation axis of a compact object (in which spatial gradients of physical and kinematic variables may be regarded as negligible). The resulting Einstein–Maxwell field equations were transformed into a system of non–linear autonomous evolution equations, which were solved numerically in the collapsing regime for a chemical potential: $\mu = 2m_e$, a magnetic field in the range $B \sim 10^7 - 10^8\text{G}$ and temperatures $T \sim 10^3 - 10^7\text{K}$.

For all initial conditions that we considered the gas evolves into a collapsing singularity, which can be (depending on the initial conditions) isotropic (“point–like”) or anisotropic (“cigar–like”). We found that for lower initial values of the magnetic field and temperatures ($B \sim 10^8\text{G}, T \sim 10^3\text{K}$) the resulting singularity is always point–like singularity, independently of the initial values of the shear. This result may be connected with the stability of volume elements in less idealized configurations, an issue that is outside the scope of this paper and deserves a proper examination elsewhere.

The collapse time decreases as the initial magnetic field increases, but we did not find a direct proportionality relation between this time and the initial temperature (this may be a consequence of having assumed a high density regime). The behavior of the temperature as the collapse proceeds also depends on initial conditions: for initial temperatures $T \sim 10^3 - 10^6\text{K}$ the gas cools down and for values $T \gtrsim 10^7\text{K}$ the temperature increases.

Using the numerical solutions of the system we found a monotonic relation between the magnetization and the magnetic field and between the energy density and the temperature for high temperature values, but relation does not occur for low temperature values. This difference in behavior can be explained by the predominance of the magnetic effects at low temperatures, though it may also be due to the limitations introduced by assuming an equation of state and a thermodynamical potential based on a one–loop approximation. Looking at this issue is beyond the scope of this paper and will be pursued in a separate work.

The study we have presented can be readily applied to examine hadronic systems (complying with suitable balance conditions and adequate chemical potentials). The methodology we have used can also serve as starting point to study the origin and the dynamics of primordial cosmological magnetic fields. These potential extensions of the present work are already under consideration for future articles.

8. Acknowledgements

The work of A.P.M, A.U.R and I.D has been supported by *Ministerio de Ciencia, Tecnología y Medio Ambiente* under the grant CB0407 and the ICTP Office of External Activities through NET-35. APM acknowledges to Prof R. Ruffini for his hospitality and financial support at International Center for Relativistic Astrophysics Network-ICRANET. A.P.M. also acknowledges the Program of Associateship TWAS-UNESCO-CNPq as well as the hospitality and support of CBPF through the program PCI-MCT. R.A.S. and A.U.R. acknowledge support from the research grant *SEP-CONACYT-132132*, and the TWAS-CONACYT fellowships.

Appendix A. Transformation of the integrals

The definitions of Γ_{\parallel} , Γ_{\perp} , Γ_U , Γ_{η} are given by equations (6)-(8), together with the coefficients (9)-(12). Hence, their derivatives take the following form:

$$\Gamma_{U,\beta} = \left[\frac{1}{2} C_3(\mu, \phi) + \sum_{n=1}^{\infty} a_n^2 C_3\left(\frac{\mu}{a_n}, \frac{\phi}{a_n}\right) \right] + \beta \sum_{n=1}^{\infty} n \left[2C_3\left(\frac{\mu}{a_n}, \frac{\phi}{a_n}\right) - \frac{a_n}{\phi} C_6\left(\frac{\mu}{a_n}, \frac{\phi}{a_n}\right) \right], \quad (\text{A.1})$$

$$\Gamma_{U,\phi} = \frac{\beta}{\phi^2} \left\{ \frac{1}{2} [C_6(\mu, \phi) - \mu C_5(\mu, \phi)] + \sum_{n=1}^{\infty} a_n^2 \left[a_n C_6\left(\frac{\mu}{a_n}, \frac{\phi}{a_n}\right) - \mu C_5\left(\frac{\mu}{a_n}, \frac{\phi}{a_n}\right) \right] \right\}, \quad (\text{A.2})$$

$$\Gamma_{U,\mu} = \frac{\beta}{\phi} \left\{ \frac{1}{2} C_5(\mu, \phi) + \sum_{n=1}^{\infty} a_n^2 C_5\left(\frac{\mu}{a_n}, \frac{\phi}{a_n}\right) \right\}, \quad (\text{A.3})$$

$$\Gamma_{\eta,\beta} = \frac{\beta}{\phi} \left[\frac{1}{2} C_4(\mu, \phi) + \sum_{n=1}^{\infty} a_n C_4\left(\frac{\mu}{a_n}, \frac{\phi}{a_n}\right) \right] + \beta \sum_{n=1}^{\infty} n \left[\frac{1}{a_n} C_4\left(\frac{\mu}{a_n}, \frac{\phi}{a_n}\right) - \frac{1}{\phi} C_5\left(\frac{\mu}{a_n}, \frac{\phi}{a_n}\right) \right], \quad (\text{A.4})$$

$$\Gamma_{\eta,\phi} = \frac{\beta}{\phi^2} \left\{ \frac{1}{2} [C_5(\mu, \phi) - \mu C_7(\mu, \phi)] + \sum_{n=1}^{\infty} a_n \left[a_n C_5\left(\frac{\mu}{a_n}, \frac{\phi}{a_n}\right) - \mu C_7\left(\frac{\mu}{a_n}, \frac{\phi}{a_n}\right) \right] \right\}, \quad (\text{A.5})$$

$$\Gamma_{\eta,\mu} = \frac{\beta}{\phi} \left\{ \frac{1}{2} C_7(\mu, \phi) + \sum_{n=1}^{\infty} a_n C_7\left(\frac{\mu}{a_n}, \frac{\phi}{a_n}\right) \right\}, \quad (\text{A.6})$$

where the coefficients C_5 , C_6 , C_7 are given by:

$$C_5(\mu, \phi) = \int_0^{\infty} h\left(\frac{\sqrt{1+x^2}-\mu}{\phi}\right) \frac{1}{\sqrt{1+x^2}} dx, \quad (\text{A.7})$$

$$C_6(\mu, \phi) = \int_0^{\infty} \frac{x^2}{\sqrt{1+x^2}} h\left(\frac{\sqrt{1+x^2}-\mu}{\phi}\right) dx, \quad (\text{A.8})$$

$$C_7(\mu, \phi) = \int_0^{\infty} h\left(\frac{\sqrt{1+x^2}-\mu}{\phi}\right) dx, \quad (\text{A.9})$$

while $h(x) = 1/(4 \cosh^2(x/2))$. The integrals (9)-(12), (A.7)-(A.9) take the form:

$$C_i(\phi, \mu) = \begin{cases} \int_0^{\infty} f_i(x) \frac{1}{1+\exp\left(\frac{\sqrt{1+x^2}-\mu}{\phi}\right)} dx, & i = \overline{1,4}, \\ \int_0^{\infty} f_i(x) h\left(\frac{\sqrt{1+x^2}-\mu}{\phi}\right) dx, & i = \overline{5,7}. \end{cases} \quad (\text{A.10})$$

Integrating by parts and making a change of variables $\nu = [\sqrt{1+x^2} - \mu]/\phi$ we finally obtain:

$$C_i(\phi, \mu) = \begin{cases} \int_{-\frac{\mu-1}{\phi}}^{\infty} F_i \left(\sqrt{(\phi\nu + \mu)^2 - 1} \right) h(\nu) d\nu, & i = \overline{1,4}, \\ \int_{-\frac{\mu-1}{\phi}}^{\infty} F_i \left(\sqrt{(\phi\nu + \mu)^2 - 1} \right) H(\nu) d\nu, & i = \overline{5,7}, \end{cases} \quad (\text{A.11})$$

with

$$F_i(x) = \int_0^x f(y) dy, \quad h(\nu) = [4 \cosh^2(\nu/2)]^{-1}, \quad H(\nu) = \frac{e^\nu(e^\nu+1)}{(e^\nu+1)^3}. \quad (\text{A.12})$$

References

- [1] Stuart L. Shapiro, Saul A. Teukolsky. 1983 "Black Holes, White Dwarfs, and Neutron Stars" ed John Wiley & Sons, Inc.
- [2] S. Chakrabarty, Phys. Rev. D **43** (1991) 627.
- [3] S. Chakrabarty, Phys. Rev. D **54** (1996) 1306 [hep-ph/9603406].
- [4] M. Chaichian, S. S. Masood, C. Montonen, A. Perez Martinez and H. Perez Rojas, Phys. Rev. Lett. **84** (2000) 5261 [hep-ph/9911218].
- [5] C. Y. Cardall, M. Prakash and J. M. Lattimer, Astrophys. J. **554** (2001) 322 [astro-ph/0011148].
- [6] R. G. Felipe, H. J. Mosquera Cuesta, A. Perez Martinez and H. Perez Rojas, Chin. J. Astron. Astrophys. **5** (2005) 399 [astro-ph/0207150].
- [7] A. Perez Martinez, H. Perez Rojas and H. Mosquera Cuesta, Int. J. Mod. Phys. D **17** (2008) 2107 [arXiv:0711.0975 [astro-ph]].
- [8] L. Paulucci, E. J. Ferrer, V. de la Incera and J. E. Horvath, Phys. Rev. D **83** (2011) 043009 [arXiv:1010.3041 [astro-ph.HE]].
- [9] A. P. Martínez, H. P. Rojas and H. J. Mosquera Cuesta, Eur. Phys. J. C **29**, 111 (2003).
- [10] R. G. Felipe and A. P. Martínez, J. Phys. G **36** (2009) 075202 [arXiv:0812.0337 [astro-ph]].
- [11] E. J. Ferrer, V. de la Incera, J. P. Keith *et al.*, Phys. Rev. C **82**, 065802 (2010).
- [12] R. G. Felipe, D. M. Paret and A. P. Martínez, Eur. Phys. J. A **47** (2011) 1 [arXiv:1003.3254 [astro-ph.HE]].
- [13] A. Ulacia Rey, A. Perez Martinez and R. A. Sussman, Gen. Rel. Grav. **40** (2008) 1499 [arXiv:0708.0593 [gr-qc]].
- [14] A. Ulacia Rey, A. Perez Martinez and R. A. Sussman, Int. J. Mod. Phys. D **16** (2007) 481 [gr-qc/0605054].
- [15] D. Manreza Paret, A. Perez Martinez, A. Ulacia Rey and R. A. Sussman, JCAP **1003** (2010) 017 [arXiv:0812.2508 [gr-qc]].
- [16] H. Y. Chiu, V. Canuto, and L. Fassio-Canuto, Phys. Rev. **176** (1968) 1438; V. Canuto and H. Y. Chiu, Phys. Rev. **173** (1968) 1229; V. Canuto and H. Y. Chiu, Phys. Rev. **173** (1968) 1220; V. Canuto, and H. Y. Chiu, Phys. Rev. **173** (1968) 1210
- [17] M. Chaichian, S. S. Masood, C. Montonen, A. Perez Martinez and H. Perez Rojas, Phys. Rev. Lett. **84** (2000) 5261 [hep-ph/9911218].
- [18] Charles. W. Misner, Kip. S. Thorne, John. Archibald. Wheeler, "Gravitation," Edit: W. H. Freeman NY, 1998.
- [19] J. Wainwright, G. F. R. Ellis, "Dynamical system in cosmology," ed Cambridge University Press, 1997.
- [20] D. Ebert, K. G. Klimenko, M. A. Vdovichenko and A. S. Vshivtsev, Phys. Rev. D **61** (2000) 025005 [hep-ph/9905253]; D. Ebert and K. G. Klimenko, Nucl. Phys. A **728** (2003) 203 [hep-ph/0305149].
- [21] C. O. Dib and O. Espinosa, Nucl. Phys. B **612** (2001) 492.
- [22] A. Ayala, A. Sanchez, G. Piccinelli and S. Sahu, Phys. Rev. D **71** (2005) 023004 [hep-ph/0412135].